

Spin-phonon coupling in van der Waals antiferromagnet VOCl

Wen-Jun Wang(王文君), Xi-Tong Xu(许锡童), Jie Shen(沈洁), Zhe Wang(王哲), Shi-Le Zhang(张仕乐), and Zhe Qu(屈哲)

Citation: Chin. Phys. B, 2021, 30 (**10**): 107502. DOI: 10.1088/1674-1056/ac041f
Journal homepage: http://cpb.iphy.ac.cn; http://iopscience.iop.org/cpb

What follows is a list of articles you may be interested in

Insights into the regulation mechanism of ring-shaped magnetoelectric energy harvesters via mechanical and magnetic conditions

Yang Shi(师阳), Ni Li(李妮), and Yong Yang(杨勇)
Chin. Phys. B, 2021, 30 (**10**): 107503. DOI: 10.1088/1674-1056/abeee9

Magnetostriction and spin reorientation in ferromagnetic Laves phase $Pr(Ga_xFe_{1-x})_{1.9}$ compounds

Min-Yu Zeng(曾敏玉), Qing Tang(唐庆), Zhi-Wei Mei(梅志巍), Cai-Yan Lu(陆彩燕), Yan-Mei Tang(唐妍梅), Xiang Li(李翔), Yun He(何云), and Ze-Ping Guo(郭泽平)
Chin. Phys. B, 2021, 30 (**6**): 067504. DOI: 10.1088/1674-1056/abe1a3

Evolution of domain structure in Fe_3GeTe_2

Siqi Yin(尹思琪), Le Zhao(赵乐), Cheng Song(宋成), Yuan Huang(黄元), Youdi Gu(顾有地), Ruyi Chen(陈如意), Wenxuan Zhu(朱文轩), Yiming Sun(孙一鸣), Wanjun Jiang(江万军), Xiaozhong Zhang(章晓中), and Feng Pan(潘峰)
Chin. Phys. B, 2021, 30 (**2**): 027505. DOI: 10.1088/1674-1056/abd693

Room-temperature ferromagnetism observed in Nd-doped In_2O_3 dilute magnetic semiconducting nanowires

Zhanpeng Lv(吕占朋), Junran Zhang(张军然), Wei Niu(钮伟), Minhao Zhang(张敏昊), Li Song(宋丽), Hairong Zhu(朱海荣), Xuefeng Wang(王学锋)
Chin. Phys. B, 2016, 25 (**9**): 097502. DOI: 10.1088/1674-1056/25/9/097502

The variation of Mn-dopant distribution state with *x* and its effect on the magnetic coupling mechanism in $Zn_{1-x}Mn_xO$ nanocrystals

Cheng Yan, Hao Wei-Chang, Li Wen-Xian, Xu Huai-Zhe, Chen Rui, Dou Shi-Xue
Chin. Phys. B, 2013, 22 (**10**): 107501. DOI: 10.1088/1674-1056/22/10/107501

Spin–phonon coupling in van der Waals antiferromagnet VOCl*

Wen-Jun Wang(王文君)[1,2], Xi-Tong Xu(许锡童)[1,3], Jie Shen(沈洁)[1,2], Zhe Wang(王哲)[1,2], Shi-Le Zhang(张仕乐)[1], and Zhe Qu(屈哲)[1,3,†]

[1] *Anhui Province Key Laboratory of Condensed Matter Physics at Extreme Conditions, High Magnetic Field Laboratory, Hefei Institutes of Physical Sciences, Chinese Academy of Sciences, Hefei* 230031, *China*

[2] *Science Island Branch of Graduate School, University of Science and Technology of China, Hefei* 230026, *China*

[3] *CAS Key Laboratory of Photovoltaic and Energy Conservation Materials, Hefei Institutes of Physical Sciences, Chinese Academy of Sciences, Hefei* 230031, *China*

(Received 11 February 2021; revised manuscript received 8 March 2021; accepted manuscript online 24 May 2021)

We report magnetization and Raman spectroscopy study on single crystals of VOCl, a van der Waals antiferromagnetic material. Magnetization measurement confirms an antiferromagnetic transition at 79 K and a magnetic easy axis along crystallographic *a* direction. The temperature-dependent Raman spectrum reveals five peaks at 30 K. Below the Neel temperature T_N, the Raman-active modes 247 cm^{-1} and 404 cm^{-1} remarkably deviate from the standard Boltzmann function, which is ascribed to the strong magnetoelastic coupling between spins and phonons. We further observe an anomaly in 383 cm^{-1} mode at around 150 K. This coincides with the broad maximum in VOCl's magnetic susceptibility, suggesting a development of short-ranged magnetic order at this temperature.

Keywords: vdW material, 2D magnetism, Raman spectroscopy, spin–phonon coupling

PACS: 75.80.+q, 78.30.–j, 63.20.–e, 96.15.Gh **DOI:** 10.1088/1674-1056/ac041f

1. Introduction

Since the discovery of single-layer graphene, two-dimensional (2D) materials have attracted tremendous research focuses. Of particular interest is the 2D magnetic material, which can host strongly enhanced spin fluctuations, surface spin contributions, large magnetic moments, and less orbital moment quenching.[1–6] It was theoretically proposed that there exists no 2D long-range magnetic ordering in the isotropic Heisenberg model.[7] However, in real material systems, magnetic anisotropy enables the presence of a spin-wave excitation gap to exhibit intrinsic magnetic ordering at finite temperatures. For example, $Cr_2Ge_2Te_6$ exhibits ferromagnetic semiconducting state in the 2D layer form.[8] Thin flake CrI_3 has long-range magnetic order which can be controlled by the number of layers.[9] Two-dimensional magnets are also susceptible to external stimuli including electric field or electrostatic doping, pressure or strain, proximity effect, etc.,[10–17] which are significant to obtain desired properties by designing intentionally.

Transition-metal oxychlorides *M*OCl (M = Ti, V, Cr and Fe) is a new family of van der Waals (vdW) antiferromagnetic materials. It features stacking layers of Cl–M_2O_2–Cl sandwiches which are connected by the weak interlayer vdW interaction. According to the previous study, this family has low exfoliation energy, large spin polarization and thickness dependent magnetic order.[18] These four *M*OCl compounds possess a rich variety of physical properties. Among them, TiOCl behaves like a quasi-one-dimensional magnetic system due to the orbital order from a single 3d electron in Ti^{3+} ions. Upon cooling, it undergoes two phase transitions: an incommensurately modulated state at 90 K and a transformation towards the spin-Peierls state at 67 K.[19] Other members' magnetic structures are 2D-like.[20,21] For instance, CrOCl has a $3d^3$ electronic configuration and a fourfold magnetic superstructure. The phase transition of CrOCl towards AFM order is observed at 13.5 K, accompanied by an *a*-axis monoclinic lattice distortion.[21] Interestingly, VOCl has a relatively high T_N (80 K)[22] and the largest monoclinic angle (90.02°, 90.22°, 90.07°, 90.09° for Ti, V, Cr, Fe, respectively) in the family,[21,23–25] which is likely due to a strong coupling between spins and phonons.

In this work, we focus on the magnetoelastic property of VOCl. High quality VOCl single crystals are synthesized via a chemical vapor transport (CVT) method. Using combined magnetization and Raman spectroscopy studies, we confirm that the phase transition point of VOCl is 79 K and the easy axis is along the direction of *a* axis. The strong coupling between the magnetic and lattice degrees of freedom is evidenced in the temperature dependence of the main Raman modes. Using Heisenberg's spin–spin correlation function $\langle S_i \cdot S_j \rangle$, the coupling constants are estimated to be as high as 3 cm^{-1} for the 247 cm^{-1} active mode, rendering VOCl as a potential candidate for application in magnetoelastic devices. We further identify a downward trend in 383 cm^{-1} mode below 150 K. This temperature corresponds to the broad maximum in magnetic susceptibility, suggesting a simultaneous de-

*Project supported by the National Natural Science Foundation of China (Grant Nos. U2032213, U1832214, and 11774352).

†Corresponding author. E-mail: zhequ@hmfl.ac.cn

© 2021 Chinese Physical Society and IOP Publishing Ltd

velopment of phonon-assisted short-ranged magnetic order in the 2D magnetic lattices.

2. Method

VOCl single crystals were synthesized by the CVT method.[26] Mixtures of V_2O_3 (97%, Sigma Aldrich) and VCl_3 (99.9%, Sigma Aldrich) with a molar ratio of 1:2 were put into a quartz tube (length 150 mm, diameter 15 mm) which was then sealed and placed in a two-temperature-zone tube furnace. The tube was heated at a rate of 1 K/min until establishing a temperature gradient of 993–893 K. Samples were transported from the hot end to the cold end for a period of seven days, and finally cooled down to room temperature naturally. The resulting dark grey VOCl crystals were washed with alcohol several times to remove residual VCl_3. Several rectangle, plate-like crystals with a typical size of 1×3 mm^2 can be obtained, as shown in the inset of Fig. 1. Powder x-ray diffraction (XRD) measurement was performed in a Rigaku x-ray diffractometer. The reflection peak positions match well with the PDF#23-1472, as shown in Fig. 1. Specific heat was measured on several single crystals stacked along the c axis using a Quantum Design PPMS. Magnetic susceptibility was conducted with a superconductive quantum interference devices (SQUID). Temperature-dependent Raman spectroscopic measurements were performed on a freshly cleaved sample employing a 532 nm solid-state laser with 2 mW for excitation in the temperature range from 20 K to 300 K. The exposure time was set as 200 s.

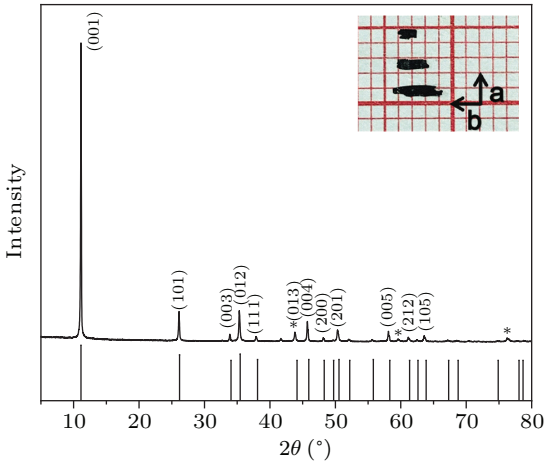


Fig. 1. XRD pattern for VOCl powders at room temperature. The extra peaks (marked by asterisks) may come from the oxides of vanadium formed during growth. Inset: image of VOCl single crystals grown by the CVT method.

3. Results and discussion

VOCl is a typical MOCl, which has orthorhombic structure at room temperature (Fig. 2(b), space group $Pmmn$, $a =$ 3.78 Å, $b = 3.30$ Å, $c = 7.91$ Å).[22] Each V^{3+} has two 3d electrons, and is located in the center of a twisted octahedra consisting of VO_4Cl_2. These are connected together to form a quasi-2D bilayer in the ab plane. Each layer is coupled with van der Waals force in crystallographic c direction. Magnetic measurement and powder neutron diffraction results have shown that VOCl is AFM below 80 K.[22,24] XRD results also suggest a lattice distortion towards a low temperature phase $P2/n$ at this temperature.[27]

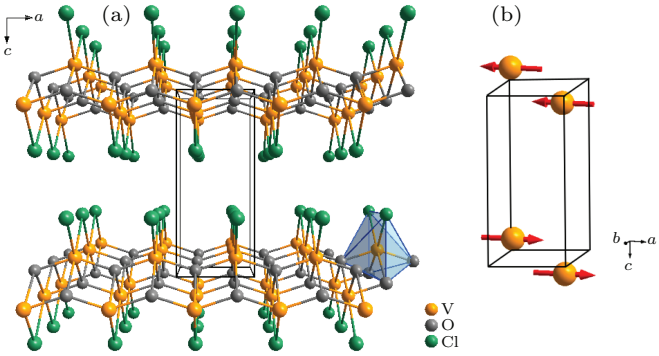


Fig. 2. (a) Room-temperature crystal structure of VOCl and the distorted VO_4Cl_2 octahedron. (b) Magnetic structure of VOCl reflected by magnetic moments of V sublattice, showing an easy a axis AFM order.

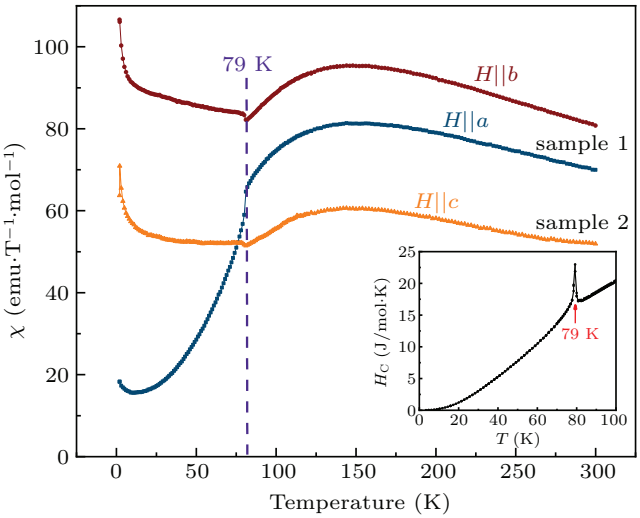


Fig. 3. Magnetic susceptibility versus temperature along the three crystallographic axes. Inset: specific heat of VOCl crystal, showing a peak at 79 K.

To study the magnetic behavior in VOCl single crystals, magnetization measurements were carried out with an applied field of 1 kOe. Figure 3 shows magnetic susceptibility χ as a function of temperature along the three crystallographic axes. The susceptibility of the a axis sharply drops below 79 K, while those of the b and c axes show a sudden rise. Combined with the built-in specific heat result, we conclude that in our samples, an AFM phase transition occurs at 79 K, with an easy a axis anisotropy. This is consistent with the previous experimental results.[22,28] We also observe a broad maximum in the vicinity of 150 K in all three directions, deviating from the Curie–Weiss behavior. This is a phenomenon often found in low-dimensional materials such as $CuGeO_3$, $Sr_{14}Cu_{24}O_{41}$ and Cu_2OCl_2,[29–31] reflecting strong 2D antiferromagnetic correlations in VOCl.[22,32] The rapid increase of the magnetic sus-

ceptibility below 10 K indicates the existence of paramagnetic impurities.

In order to study the connection between AFM ordering and atomic vibrations in VOCl, we now focus on measured Raman spectrum over the frequency range from 100 to 650 cm^{-1}. Figure 4 shows the identified five Raman modes at 30 K, including three strong phonon modes ($p1$, $p3$, $p4$)[33] and two weak ones ($p2$, $p5$). These modes are ascribed to the stretching vibrations of V–Cl bonds.[34] The number of visible Raman modes is less than the previous report,[34] which may be ascribed to purity and defections of different crystals, the accidental degeneracy of several neighboring phonon frequencies or intensity reduction of several phonons due to smaller polarizability.[35] All these Raman peaks get smaller and wider as the temperature increases, due to enhanced phonon vibration and scattering. The peak near 630 cm^{-1} ($p5$) at low temperatures is indistinguishable above 240 K due to its weak intensity.

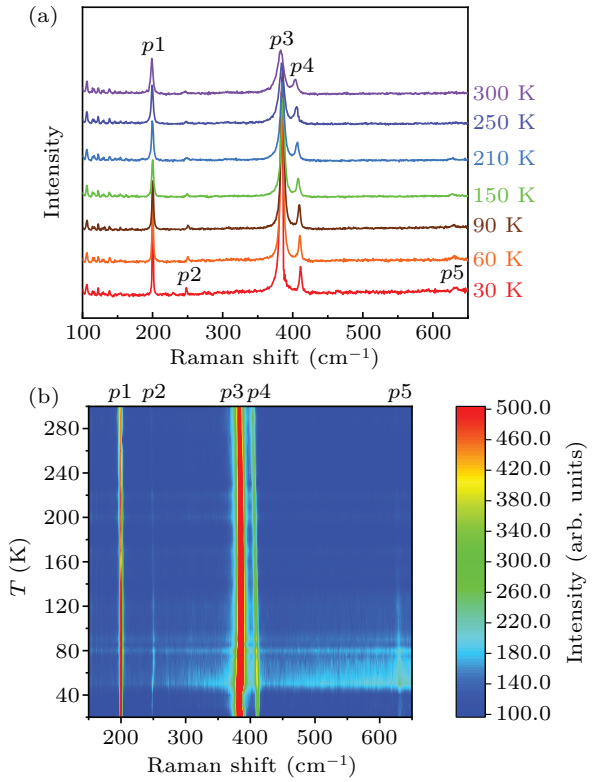


Fig. 4. (a) Raman spectrum over the frequency range 100–650 cm^{-1} at several typical temperatures. Five discernable peaks are labeled with $p1$ to $p5$, respectively. (b) Corresponding colormap of the Raman spectrum.

For all these five modes, no abrupt changes are observed across the Neel temperature, which is consistent with the previous suggestion that the monoclinic lattice distortion is solely driven by the magnetic interactions.[27]

The temperature dependence of the peak positions of the four major modes ($p1$ to $p4$) is shown in Fig. 5. Many factors can contribute to mode frequency, such as lattice anharmonicity originated from the displacement between atoms, quasi-harmonicity, electron-phonon coupling, and spin–phonon coupling effect.[35] Thus, the following relation can be obtained:

$$\omega(T) = \omega_0 + \Delta\omega(T)_{\text{s-p}} + \Delta\omega(T)_{\text{qh}} + \Delta\omega(T)_{\text{anh}} + \Delta\omega(T)_{\text{el-ph}},$$

where ω_0 is the phonon frequency at absolute zero temperature, ω_{qh} represents the quasi-harmonic contribution, ω_{anh} corresponds to the contribution from phonon–phonon interaction, $\omega_{\text{el-ph}}$ and $\omega_{\text{sp-ph}}$ are the electron–phonon and the spin–phonon coupling effect. As VOCl is a insulator, there is no electron–phonon coupling effect. The quasi-harmonic contribution is significant only when the distance between atoms varies, while from synchrotron-radiation powder x-ray diffraction measurements,[24] the change in unit cell volume from 15 K to 300 K is found to be only about 0.83%. Thus the part from ω_{qh} is also ruled out. We therefore conclude only the contributions from lattice anharmonicity and spin–phonon couple effect may work on the mode frequencies in VOCl. In the paramagnetic phase, the lattice anharmonicity governs the evolution of mode frequency. We can use the Boltzmann function to describe the nature of crystals

$$\omega(T) = \frac{\omega_0 - \omega_1}{1 + \exp\left(\dfrac{T - T_0}{\mathrm{d}T}\right)} + \omega_1,$$

where ω_1 and ω_0 are high-temperature and low-temperature limit values of phonon frequency, T_0 is the center point (the point with the largest rate of change), and $\mathrm{d}T$ is a temperature characteristic quantity from the lowest value to the highest value. We plot all fitted curves shown in Fig. 5. The profile of 199 cm^{-1} ($p1$) mode frequency roughly follows the fitting curve in our measured temperature range, suggesting that $p1$ is barely affected by magnetic order. The 247 cm^{-1} ($p2$) and 404 cm^{-1} ($p4$) modes, on the other hand, show a strong deviation from Boltzmann fitting results below T_{N}, indicating a large contribution from spin–phonon coupling. It is worth noticing that the deviation of 383 cm^{-1} ($p3$) occurs at 150 K, well above the Neel temperature of VOCl. This temperature also corresponds to the broad maximum in the susceptibility curve in Fig. 3. Note that in the 2D Heisenberg antiferromagnet model,[35] this maximum arises from spin correlations of nearest neighbors. We therefore give evidence that a short-range magnetic order, which is strongly coupled to phonons, develops around 150 K in VOCl.

The deviation from the Boltzmann function can be used to estimate the strength of spin–phonon coupling at zero temperature via $\omega_{\text{sp-ph}} = \lambda\langle S_i \cdot S_j\rangle$,[36] where λ is the spin–phonon coupling constant related to the magnetic exchange, and $\langle S_i \cdot S_j\rangle$ is spin-spin correlation function. As V^{3+} is the only magnetic ion at 0 K, the value of $\langle S_i \cdot S_j\rangle$ can be defined as S^2.[37] Without regard to the sign of the frequency shift, λ is found to be 3 cm^{-1}, 2 cm^{-1}, 1.2 cm^{-1} for the $p2$, $p3$ and $p4$ modes, respectively. The spin–phonon coupling constant of VOCl is larger than many 2D materials with magnetoelastic effect, such as $Cr_2Ge_2Te_6$ (λ = 1.2 cm^{-1}), $CrSiTe_3$

($\lambda = 0.2$ cm^{-1}), $CrCl_3$ ($\lambda = 0.9$ cm^{-1}), $[Cu(pyz)_2(HF_2)]PF_6$ ($\lambda = 2$ cm^{-1}).[37–40] The large value of λ making VOCl a potential candidate for applications in low-dimensional magnetoelastic devices. The reason behind such a remarkable spin–phonon coupling in a short-ranged magnetic order for $p3$ mode deserves future studies.

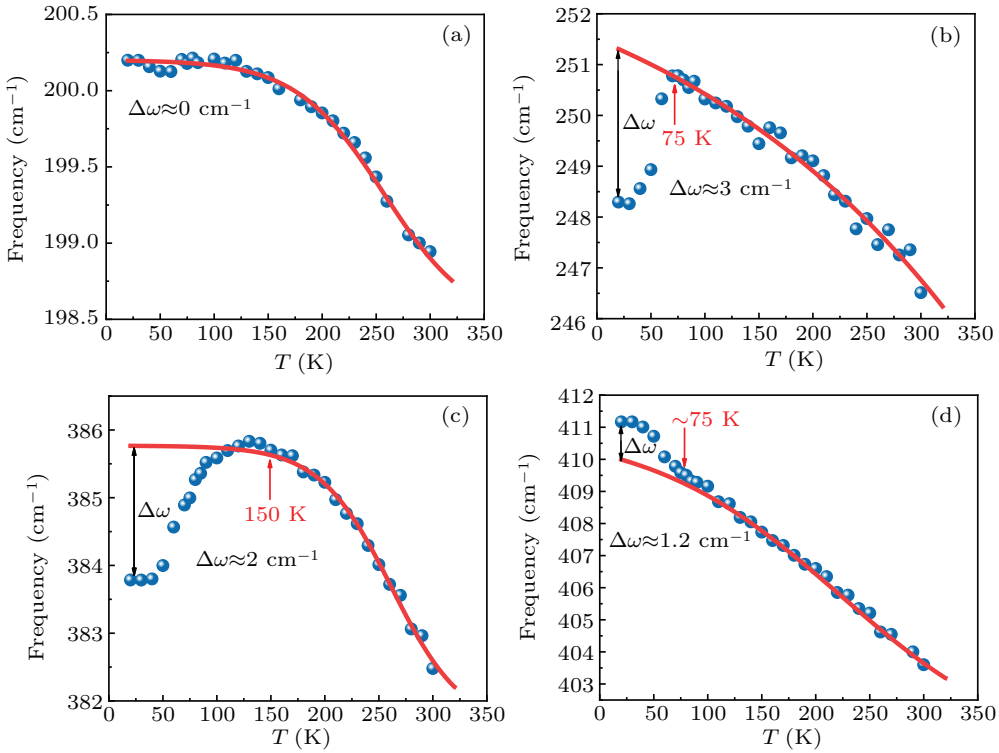


Fig. 5. Frequencies versus temperature for main modes at (a) 199 cm^{-1}, (b) 247 cm^{-1}, (c) 383 cm^{-1}, (d) 404 cm^{-1}, respectively. Data are fitted with the Boltzmann function illustrated by the solid red line, suggesting a spin–lattice coupling.

4. Conclusion

In conclusion, we have studied the magnetization behavior and temperature dependence of Raman spectroscopy of VOCl single crystals. The magnetic susceptibility of the a axis sharply drops below 79 K, which implies an AFM magnetic order along a direction. Raman spectroscopy identifies three strong phonon modes ($p1$, $p3$, $p4$) and two weak phonon modes ($p2$, $p5$) at 30 K. The temperature dependence of the four modes is studied in detail. Below T_N, the Raman-active mode $p1$ at 199 cm^{-1} is barely changed, while $p2$ and $p4$ (247 cm^{-1} and 404 cm^{-1}, respectively) show remarkable deviations, which is ascribed to the strong magnetoelastic coupling between spins and phonons for these two modes. Furthermore, we report a decrease of the $p3$ (383 cm^{-1}) mode below 150 K, which is likely due to the development of short-ranged magnetic order above T_N. Our results reveal the existence of a strong coupling between spins and lattices, which is crucial for understanding the 2D magnetism in VOCl.

References

[1] Sethulakshmi N, Mishra A, Ajayan P M, Kawazoe Y, Roy A K, Singh A K and Tiwary C S 2019 *Mater. Today* **27** 107

[2] Moriya T, Takahashi Y and Ueda K 1990 *J. Phys. Soc. Jpn.* **59** 2905

[3] Birgeneau R, Aharony A, Belk N, Chou F, Endoh Y, Greven M, Hosoya S, Kastner M, Lee C and Lee Y 1995 *J. Phys. Chem. Solids* **56** 1913

[4] Siegmann H 1992 *J. Phys.: Condens. Matter* **4** 8395

[5] Ashton M, Gluhovic D, Sinnott S B, Guo J, Stewart D A and Hennig R G 2017 *Nano Lett.* **17** 5251

[6] Freeman A J and Fu C 1987 *J. Appl. Phys.* **61** 3356

[7] Mermin N D and Wagner H 1966 *Phys. Rev. Lett.* **17** 1133

[8] Gong C, Li L, Li Z, *et al.* 2017 *Nature* **546** 265

[9] Huang B, Clark G, Navarro-Moratalla E, *et al.* 2017 *Nature* **546** 270

[10] Zhong D, Seyler K L, Linpeng X, *et al.* 2017 *Sci. Adv.* **3** e1603113

[11] Wang Z, Zhang T, Ding M, *et al.* 2018 *Nat. Nanotechnol.* **13** 554

[12] Wang X R, Si Y and Zhang R 2013 *Chin. Phys. B* **22** 098505

[13] Jiang S, Li L, Wang Z, Mak K F and Shan J 2018 *Nat. Nanotechnol.* **13** 549

[14] Ma Y, Dai Y, Guo M, Niu C, Zhu Y and Huang B 2012 *ACS Nano* **6** 1695

[15] Cummings A W, Garcia J H, Fabian J and Roche S 2017 *Phys. Rev. Lett.* **119** 206601

[16] Song K, Soriano D, Cummings A W, Robles R, Ordejón P and Roche S 2018 *Nano Lett.* **18** 2033

[17] Liang F, Xu H, Wu X, Wang C, Luo C and Zhang J 2018 *Chin. Phys. B* **27** 037802

[18] Miao N, Xu B, Zhu L, Zhou J and Sun Z 2018 *J. Am. Chem. Soc.* **140** 2417

[19] Rückamp R, Baier J, Kriener M, Haverkort M, Lorenz T, Uhrig G, Jongen L, Möller A, Meyer G and Grüninger M 2005 *Phys. Rev. Lett.* **95** 097203

[20] Kauzlarich S, Ellena J, Stupik P, Rieff W and Averill B 1987 *J. Am. Chem. Soc.* **109** 4561

[21] Angelkort J, Wölfel A, Schönleber A, van Smaalen S and Kremer R K 2009 *Phys. Rev. B* **80** 144416

[22] Wiedenmann A, Rossat-Mignod J, Venien J and Palvadeau P 1984 *J. Magn. Magn. Mater.* **45** 275

[23] Schönleber A, Shcheka G and van Smaalen S 2008 *Phys. Rev. B* **77** 094117

[24] Komarek A, Taetz T, Fernández-Díaz M, Trots D, Möller A and Braden M 2009 *Phys. Rev. B* **79** 104425
[25] Grant R 1971 *J. Appl. Phys.* **42** 1619
[26] May A F, Yan J and McGuire M A 2020 *J. Appl. Phys.* **128** 051101
[27] Schönleber A, Angelkort J, van Smaalen S, Palatinus L, Senyshyn A and Morgenroth W 2009 *Phys. Rev. B* **80** 064426
[28] Wiedenmann A, Venien J, Palvadeau P and Rossat-Mignod J 1983 *J. Phys. C: Solid State Phys.* **16** 5339
[29] Riera J and Dobry A 1995 *Phys. Rev. B* **51** 16098
[30] Matsuda M and Katsumata K 1996 *Phys. Rev. B* **53** 12201
[31] Okabe H, Suzuki K, Kawashima K, Muranaka T and Akimitsu J 2006 *J. Phys. Soc. Jpn.* **75** 123705
[32] Lines M 1970 *J. Phys. Chem. Solids* **31** 101
[33] Zhang T, Wang Y, Li H, *et al.* 2019 *ACS Nano* **13** 11353
[34] Gao P, Lin X M, Reddy M A, Zhang L, Diemant T, Behm R J and Fichtner M 2016 *J. Electrochem. Soc.* **163** A2326
[35] Mishra K, Shukla R, Krishna P, Babu P, Achary S, Katiyar R and Scott J 2020 *Phys. Chem. Chem. Phys.* **22** 6906
[36] Fennie C J and Rabe K M 2006 *Phys. Rev. Lett.* **96** 205505
[37] Casto L, Clune A, Yokosuk M, *et al.* 2015 *APL Mater.* **3** 041515
[38] Tian Y, Gray M J, Ji H, Cava R and Burch K S 2016 *2D Mater.* **3** 025035
[39] Glamazda A, Lemmens P, Do S H, Kwon Y and Choi K Y 2017 *Phys. Rev. B* **95** 174429
[40] Wahish A, O'Neal K, Lee C, *et al.* 2017 *Phys. Rev. B* **95** 104437